548

Arch. Pharm. Chem. Life Sci. 2008, *341*, 548–553

Full Paper

Synthesis of Nitroxyl Radicals for Overhauser-enhanced Magnetic Resonance Imaging

Ken-ichi Yamada[1], Yuichi Kinoshita[1], Toshihide Yamasaki[1], Hiromi Sadasue[1], Fumiya Mito[1], Mika Nagai[1], Shingo Matsumoto[1], Mariko Aso[2], Hiroshi Suemune[2], Kiyoshi Sakai[1], and Hideo Utsumi[1]

[1] Department of Bio-function Science, Faculty of Pharmaceutical Sciences, Kyushu University, Fukuoka, Japan

[2] Department of Pharmaceutical Synthetic Chemistry, Faculty of Pharmaceutical Sciences, Kyushu University, Fukuoka, Japan

Non-invasive measurement and visualization of free radicals *in vivo* would be important to clarify their roles in the pathogenesis of free radical-associated diseases. Nitroxyl radicals can react with free radicals and be derivatized to achieve specific cellular / subcellular localizing capabilities while retaining the simple spectral features useful in imaging. Overhauser-enhanced magnetic resonance imaging (OMRI), which is a double resonance technique, creates images of free radical distributions in small animals by enhancing the water proton signal intensity via the Overhauser Effect. In this study, we synthesized various nitroxyl probes having ^{15}N nuclei and deuterium, and measured the enhancement factor for Overhauser-enhanced magnetic resonance imaging experiments. ^{15}N-D-4-Oxo-2,2,6,6-tetramethylpiperidine-1-oxyl (^{15}N-D-oxo-TEMPO) has the highest enhancement factor compared with other nitroxyl probes. The proton signal enhancement was higher for ^{15}N-labeled nitroxyl probes when compared to the ^{14}N-labeled analogues because of the reduced spectral multiplicity of the I = 1/2 nucleus. Furthermore, this enhancement is proportional to the line width and number of electron spin resonance lines of nitroxyl radicals. Finally, we compared the Overhauser-enhanced magnetic resonance image of ^{15}N-labeled, deuterated 4-Oxo-2,2,6,6-tetramethylpiperidine-1-oxyl with that of ^{14}N-H-TEMPOL. These results suggested that the selective deuteration of the nitroxyl probes enhanced the signal-to-noise ratio and thereby improved spatial and temporal resolutions.

Introduction

Free radicals including reactive oxygen and nitrogen species reveal two completely different characteristics depending on the dose loaded and the situation in which each living cell is placed: namely, functional in physiological conditions, but harmful in a variety of pathological conditions. Free-radical reactions *in vivo* appear extremely complicated because there are numerous molecules and reaction pathways that might influence radical reactions. Furthermore, the oxygen concentration in most tissues *in vivo* is much lower than that in *in-vitro* experiments. Therefore, non-invasive measurement and visualization of free radicals *in vivo* would be important to clarify their roles in the pathogenesis of free radical-associated diseases.

The most direct technique available for the detection of reactive free radicals *in vivo* is electron spin resonance (ESR) spectroscopy, which requires a spin-probe

Correspondence: Hideo Utsumi Ph.D., Department of Bio-function Science, Faculty of Pharmaceutical Sciences, Kyushu University, 3-1-1 Higashi-ku, Maidashi, Fukuoka 812-8582, Japan.
E-mail: utsumi@pch.phar.kyushu-u.ac.jp
Fax: +81-92-642-6626

Abbreviations: Electron spin resonance (ESR); dynamic nuclear polarization (DNP); Overhauser-enhanced magnetic resonance imaging (OMRI); 4-Oxo-2,2,6,6-tetramethylpiperidine-1-oxyl (oxo-TEMPO); 4-hydroxyl-2,2,6,6-tetramethylpiperidine-*N*-oxyl (TEMPOL); triaryl-methyl (TAM)

Arch. Pharm. Chem. Life Sci. 2008, *341*, 548 – 553

Nitroxyl Radicals for OMRI   549

approach. The *in vivo* spin-probe technique has been used to evaluate the generation of free radicals [1–3] and the redox status [4–7] by monitoring the ESR signal loss. The reaction of nitroxyl radicals as spin-probes with free radicals is dependent on the basic structure of nitroxyl probes such as piperidine or pyrrolidine. Furthermore, nitroxyl probes can be derivatized to achieve specific cellular / subcellular localizing capabilities while retaining the simple spectral features useful in imaging. Recently, we developed a non-invasive technique to evaluate the *in vivo* free-radical generation both in and out of membranes in living animals using several spin probes with different physical properties [2, 8]. The involvement of lipid-derived free radicals was reported recently during the initiation of the nitrosamine metabolism [8].

Overhauser-enhanced magnetic resonance imaging (OMRI) is a double resonance technique that uses the presence of paramagnetic agents to enhance the signal intensity from nuclear spins via a process known as dynamic nuclear polarization (DNP) or Overhauser Effect [9–12]. In this phenomenon, the relatively stronger magnetic moment of the electron is utilized to enhance the polarization of the nuclear spins, thereby enhancing their signal. The unique advantage of this technique is high spatial resolution of the image and short acquisition time. The significant contrast-to-noise ratio obtained by this technique at very low magnetic fields for ^{1}H-based MRI detection (~10 mT) compared to the routinely used MRI systems that operate at fields ~1 T makes OMRI advantageous in obtaining physiological information. Alecci *et al*. utilized nitroxyl radicals and successfully obtained images of water protons in tissue in the vicinity of the paramagnetic radical and so achieved *in-vivo* imaging [13]. More recently, we reported that the use of ^{14}N and its isotropic compound ^{15}N nuclei to label nitroxyl radicals with OMRI, can visualize the reaction with ascorbic acid on the inner and outer membranes of liposomes [14]. Unfortunately, the utilization of nitroxyl radicals used as spin probes for OMRI experiments is restricted due to a broad-line width compared with the triarylmethyl (TAM) radical. Grucker *et al*. reported that the enhancement factor of deuterated 4-Hydroxyl-2,2,6,6-tetramethylpiperidine-1-oxyl (TEMPOL) was higher than that of TEMPOL using a DNP spectrometer [15]. Furthermore, they suggested that with the ^{15}N-labeled and deuterated compound the higher enhancement factor can be obtained because of the ^{15}N nuclei spin (I = 1/2) and the small gyromagnetic ratio of deuterium.

The aim of this study was to synthesize the various nitroxyl probes that have a ^{15}N nucleus and deuterium, and measure the enhancement factor to design the new nitroxyl probes to improve the OMRI image resolution.

Results and discussion

Chemistry

Synthesis of 2,2,6,6-tetramethyl-piperidine-4-one **1** was carried out according to the methods of a previous report [16]. The isotope-labeled compound **1** was either deuterated using acetone-d_6 or ^{15}N-labeled with ^{15}N-ammonium chloride. Isotope-labeled nitroxyl probes were synthesized by using the isotope-labeled compound **1** in the manner depicted in Scheme 1 [17–19].

Electron spin resonance measurements

The nitroxyl radical with a ^{14}N nucleus exhibited an Electron spin resonance (ESR) spectrum that exhibited a three-line spectrum characteristic of the unpaired electron interacting with the ^{14}N nucleus (I = 1), whereas the nitroxyl radical derivative with the nitrogen nucleus substituted with ^{15}N (I = ½) exhibited an ESR spectrum with a doublet with hyperfine splitting (data not shown). The reinforcement of the signal intensity of 40–50% was seen in the ^{15}N body in comparison with a ^{14}N body by a decrease in division number.

Regarding the deuterated nitroxyl probes, the ESR spectrum-line width became narrow to 70% in comparison with non-deuterated nitroxyl probes (Table 1). Because the gyromagnetic ratio of deuterium atom is 1 : 6 in comparison with hydrogen, the ESR spectrum-line width of deuterated nitroxyl probes is narrow. When the signal intensity of deuterated nitroxyl probes reinforced the shared portions, that line width became narrow.

2.3 OMRI experiments

Figures 1a and b show the corresponding DNP spectra of ^{14}N- and ^{15}N-labeled nitroxyl probes obtained by detecting the proton intensities after ESR irradiation at appropriate magnetic fields in the range of 5–10 mT. The ^{14}N-labeled nitroxyl radical has a ^{14}N nucleus that exhibits an ESR spectrum of three lines, characteristic of an unpaired electron interacting with a ^{14}N nucleus. The unequal coupling constants, which are usually observed at low-frequency measurements, are caused by breakdown of the high-field approximation, known as the"Breit-Rabi" effect. ^{15}N-labeled nitroxyl probes have ^{15}N nuclei substituted for ^{14}N nuclei; these exhibit an ESR spectrum with a doublet with hyperfine splitting. The ^{14}N and ^{15}N hyperfine coupling constants obtained from the DNP spectra for the two nitroxyls are in close agreement with the corresponding hyperfine coupling constants measured in their ESR spectra. Table 2 shows DNP signal enhancement in the presence of various nitroxyl probes in phosphate-buffered saline solution (pH = 7.4). Oxo-TEMPO (4-

**Table 1**. Line width (μT) of [14]N- and ^{15}N-labeled nitroxyl probes.

Nitroxyl Probes	^{14}N-H	^{14}N-D	^{15}N-H	^{15}N-D
Oxo-TEMPO	39.6 ± 3.02	29.9 ± 0.97	39.1 ± 1.87	31.1 ± 1.21
TEMPOL	139.7 ± 0.67	98.8 ± 3.00	151.8 ± 1.40	121.0 ± 2.88
Carbamoyl-PROXYL	114.4 ± 4.76	79.4 ± 4.78	114.4 ± 2.62	70.1 ± 1.44
Carboxy-PROXYL	126.0 ± 3.24	76.5 ± 3.45	115.8 ± 5.99	78.2 ± 2.81
MC-PROXYL	115.6 ± 7.51	80.9 ± 4.85	113.4 ± 7.71	73.7 ± 4.32

Nitroxyl probes (10 μM) were dissolved in 0.1 M phosphate-buffered saline (pH 7.4). All values represent the mean ± SD (n = 3).

Table 2. Enhancement factor of [14]N- and ^{15}N-labeled nitroxyl probes.

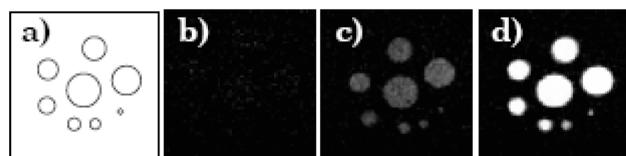| Nitroxyl Probes	^{14}N-H	^{14}N-D	^{15}N-H	^{15}N-D
Oxo-TEMPO	11.4 ± 0.75	11.6 ± 0.09	20.6 ± 0.17	23.7 ± 0.78
TEMPOL	6.5 ± 0.67	8.1 ± 0.20	13.1 ± 0.28	16.1 ± 0.87
Carbamoyl-PROXYL	7.3 ± 0.28	9.8 ± 0.09	15.4 ± 0.62	20.5 ± 0.61
Carboxy-PROXYL	7.1 ± 0.22	10.3 ± 0.30	15.6 ± 1.22	22.0 ± 1.14
MC-PROXYL	7.1 ± 0.28	9.3 ± 0.29	15.8 ± 0.44	20.6 ± 0.11

Nitroxyl probes (2 mM) were dissolved in 0.1 M phosphate-buffered saline (pH 7.4). All values represent the mean ± SD (n=3).
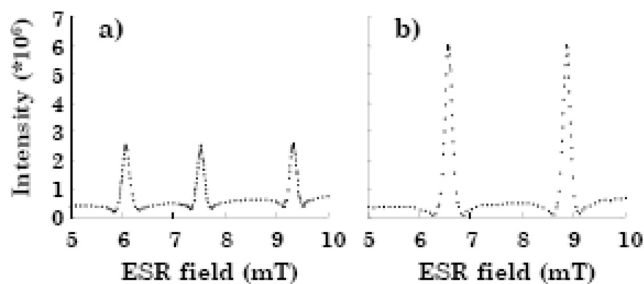
Figure 1. Dynamic nuclear polarization spectra of nitroxyl probes (2 mM). (a) ^{14}N-labeled nitroxyl radical, (b) ^{15}N-labeled nitroxyl radical.

Figure 2. Overhauser-enhanced magnetic resonance images in the presence of nitroxyl probes (2 mM). (a) The scheme of eight phantom tubes. (b) Electron spin resonance OFF image. (c) ^{14}N-H-TEMPOL image. (d) ^{15}N-D-oxo-TEMPO image. The inner diameters of the eight phantom tubes were 7, 6, 5, 4, 3, 2, 1.5, and 0.7 mm. Experimental conditions are described in Experimental, Section 3.

Oxo-2,2,6,6-tetramethylpiperidine-1-oxyl) has a higher enhancement factor compared with the other nitroxyl probes. The proton signal enhancement was higher for ^{15}N-labeled nitroxyl probes when compared to the ^{14}N-labeled analogues because of the reduced spectral multiplicity of the I = 1/2 nucleus. Furthermore, this enhancement is proportional to the line width and number of ESR lines of nitroxyl radicals (Tables 1 and 2). These results are in agreement with a previous report [20] that mentioned that the enhancement factor can be written as:

$$E = 1 - \frac{1}{n}\ \frac{r_e}{r_n}\ \rho f s \qquad (1)$$

where r_e and r_n are the electronic and nuclear gyromagnetic ratios, respectively. The other variables in Eq. (1) are ρ, the coupling factor f, the leakage factor s, the saturation factor, and n, the number of lines in the free radical's ESR spectrum. From the equation and in this experiment, the ^{15}N-labeled and deuterated nitroxyl probes give higher enhancement factors for OMRI experiments.

To examine the image conditions under which nitroxyl probes can be seen, a phantom containing a nitroxyl probe was placed in several different tubes and tested. Figure 2a shows the scheme of eight phantom tubes with different sizes of inner diameters. Figure 2b shows a phantom image that was collected in the absence of ESR irradiation yet in the presence of the nitroxyl probe; this image is characteristic of a magnetic resonance image with poor signal-to-noise ratio (SNR). The poor SNR and spatial resolution of the image are consistent with the low magnetic field (15 mT) at which the MR images were collected. Although the gross features of the phantom could be recognized, the image resolution is not sufficient to provide a sharply defined image of the phantom. The magnetic resonance images were collected after a period of ESR irradiation; examples are shown in Figs. 2c and d. The use of nitroxyl probes facilitated sig-
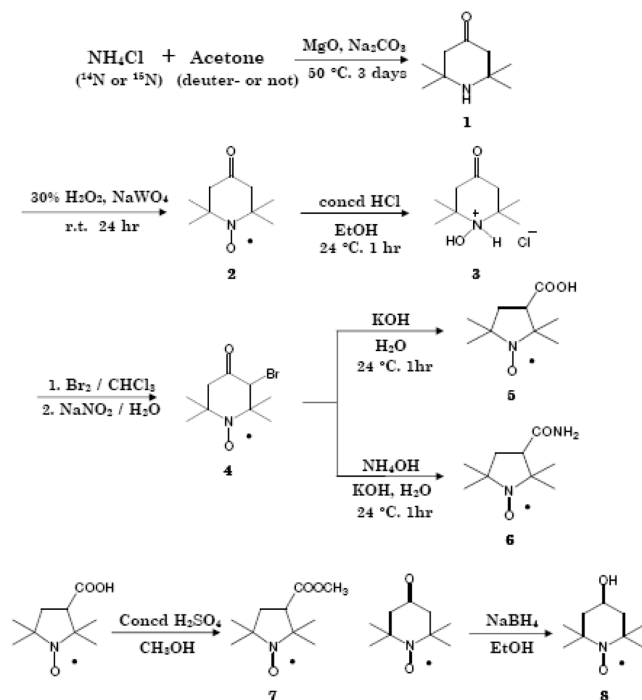
Scheme 1. Synthesis of isotope-labeled nitroxyl probes.

nificantly enhanced images. The resolution in the image was ~0.7 mm. It was found that the image intensity of ^{15}N-deuterated oxo-TEMPO, which has a narrow line width, was much higher than that of ^{14}N-H-4-hydroxyl-2,2,6,6-tetramethylpiperidine-*N*-oxyl (^{14}N-H-TEMPOL).

In conclusion, these results suggested that the selective deuteration of the nitroxyl probes enhanced the signal-to-noise ratio and thereby improved spatial and temporal resolutions. The OMRI technique is a powerful imaging modality for use in small animal research to understand the mechanism of free radical-related diseases. Progress in this field is largely conditional on the design of new nitroxyl probes.

Experimental

Materials

Ammonium chloride (^{15}N, 99%) and acetone-d_6 were obtained from Cambridge Isotope Laboratories, Inc. (Andover, MA, USA). 3-carboxy-2,2,5,5-tetramethylpyrrolidine-*N*-oxyl (carboxy-

PROXYL), 3-carbamoyl-2,2,5,5-tetramethylpyrrolidine-*N*-oxyl (carbamoyl-PROXYL), 4-oxo-2,2,6,6-tetramethylpiperidine-*N*-oxyl (oxo-TEMPO), and 4-hydroxyl-2,2,6,6-tetramethylpiperidine-*N*-oxyl (TEMPOL) were purchased from Aldrich (St. Louis, MO, USA). All other reagents were all obtained from Wako Pure Chemical Industries (Osaka, Japan). Isotope-labeled nitroxyl probes were synthesized by using the isotope-labeled 2,2,6,6-tetramethylpiperidine-4-one according to Scheme 1.

2,2,6,6-Tetramethylpiperidine-4-one (Triacetoneamine) 1

A mixture of ammonium chloride or ^{15}N-ammonium chloride (37.4 mmol), acetone, or acetone-d_6 (98.6 mmol), anhydrous sodium carbonate (173 mmol), and magnesium oxide (432 mmol) was added to a 1 L round-bottomed flask. The flask was capped with a rubber septum and wired; then, the reaction mixture was heated in an oil-bath at 50°C for three days. After cooling, 20 mL of acetone was added to the reaction mixture and the resulting solution was filtered. The recovered solid was crushed into powder, washed with 15 mL of acetone, and was then filtered with suction filtration. The combined filtrates were evaporated and purified with silica gel column chromatography. The resulting red liquid was solidified by chilling in a dry ice / acetone bath. The solid product was recrystallized with hexane to afford 97 mmol (26.0%) of a colorless crystal. Calculated for $C_9H_{17}NO$: C, 69.19; H, 10.97; N, 8.96. Found: C, 68.13; H, 10.94; N, 8.91.

4-Oxo-2,2,6,6-tetramethylpiperidine-1-oxyl (Oxo-TEMPO)

A solution of 2,2,6,6-tetramethylpiperidine-4-one (97 mmol) and sodium tungstate dihydrate (4.82 mmol) in 99.7 mL of water was cooled to 5°C and 22.3 mL of 30–35.5% hydrogen peroxide was added with stirring. The temperature did not exceed 25°C. The suspension was stirred vigorously for 24 h at ambient temperature. Then, it was saturated with potassium carbonate and extracted with ether. The ether phase was dried over magnesium sulfate, filtered, and evaporated. The residue was recrystallized from hexane to give 79.6 mmol (82.1%) of an orange product.

1-Hydroxyl-4-oxo-2,2,6,6-tetramethylpiperidine hydrochloride

Aqueous hydrochloric acid (37%, 7.65 mL) was added dropwise at 5°C to a stirred solution of 4-oxo-2,2,6,6-tetramethylpiperidine-1-oxyl (79.6 mmol) in ethanol (11 mL). The reaction mixture was stirred for 1 h at 24°C. The solvent was removed in a rotating evaporator and the residue was recrystallized from 2-propanol to give 53.9 mmol (67.7%) of a white solid. Calculated for $C_9H_{18}ClNO_2$: C, 52.05; H, 8.74; N, 6.74. Found: C, 52.07; H, 8.71; N, 6.72.

3-Bromo-4-oxo-2,2,6,6-tetramethylpiperidine-1-oxyl

A solution of bromine (53.9 mmol) in chloroform (5 mL) was added dropwise to a stirred solution of 1-hydroxyl-4-oxo-2,2,6,6-tetramethylpiperidine hydrochloride (53.9 mmol) in chloroform (110 mL). After a clear solution was observed, to this solution was added with vigorous stirring a solution of sodium nitrite (121 mmol) in water (118 mL). The mixture was stirred for 30 min at 24°C. The chloroform layer was separated, washed with water, and dried with anhydrous magnesium sulfate. After removal of the solvent in a rotating evaporator, the residue was

552   K. Yamada *et al.*

Arch. Pharm. Chem. Life Sci. 2008, *341*, 548 – 553

recrystallized from hexane to give 31.8 mmol (59%) of an orange product. Calculated for $C_9H_{15}BrNO_2$: C, 43.22; H, 6.04; N, 5.60. Found: C, 43.17; H, 6.05; N, 5.67.

3-Carboxy-2,2,5,5-tetramethylpyrrolidine-1-oxyl (Carboxy-PROXYL)

Compound 3-bromo-4-oxo-2,2,6,6-tetramethylpiperidine-1-oxyl (31.8 mmol) was added, portionwise, to a stirred solution of potassium hydroxide (79.5 mmol) in water (79.5 mL). The reaction mixture was stirred for 2 h at 24°C, acidified with 5 N aqueous hydrochloric acid solution to pH = 3, and quickly extracted with chloroform. The organic layer was dried with anhydrous magnesium sulfate. After removal of the solvent in a rotating evaporator, the residue was first purified with silica gel column chromatography and then recrystallized from a mixture of chloroform and hexane (3 / 1, v / v) to give 14.95 mmol (47%) of a yellow product.

[14N, D] IR (cm^{-1}): 2975 (-COOH), 1731 (C=O), Calculated for $C_9HD_{15}NO_3$: C, 53.65; H, 8.00; N, 6.96. Found: C, 55.07; H, 8.23; N, 7.11. [15N, H] IR (cm^{-1}): 2976 (-COOH), 1728 (C=O), Calculated for $C_9H_{16}{}^{15}NO_3$: C, 57.69; H, 8.61; N, 7.48. Found: C, 57.68; H, 8.53; N, 7.53. [15N,D] IR (cm^{-1}): 2973 (-COOH), 1730 (C=O), Calculated for $C_9HD_{15}{}^{15}NO_3$: C, 53.38; H, 7.96; N, 6.92. Found: C, 54.57; H, 8.21; N, 7.16.

3-Carbamoyl-2,2,5,5-tetramethylpyrrolidine-1-oxyl (Carbamoyl-PROXYL)

Portionwise, 3-bromo-4-oxo-2,2,6,6-tetramethylpiperidine-1-oxyl (10.6 mmol) was added to a solution of potassium hydroxide (31.0 mmol) in 29% ammonia (85.3 mL). The reaction mixture was stirred for 1 h at 24°C, and then extracted with chloroform. The chloroform layer was dried with anhydrous magnesium sulfate. After removal of the solvent in a rotating evaporator, the residue was first purified with silica gel column chromatography, and then recrystallized from acetone to give 4.24 mmol (40.0%) of a yellow product.

[14N, D] IR (cm^{-1}): 3208 – 3427 (NH), 1672 (C=O), Calculated for $C_9H_2D_{15}N_2O_2$: C, 53.91; H, 8.55; N, 13.98. Found: C, 55.67; H, 8.20; N, 14.40. [15N, H] IR (cm^{-1}): 3207 – 3428 (NH), 1678 (C=O), Calculated for $C_9H_{17}N^{15}NO_2$: C, 57.99; H, 9.20; N, 15.04. Found: C, 58.06; H, 9.17; N, 15.14. [15N, D] IR (cm^{-1}): 3201-3407 (NH), 1679 (C=O), Calculated for $C_9H_2D_{15}{}^{15}N_2O_2$: C, 53.64; H, 8.50; N, 13.91. Found: C, 55.18; H, 8.81; N, 14.30.

3-Methoxycarbonyl-2,2,5,5-tetramethylpyrrolidine-1-oxyl (MC-PROXYL)

Concentrated sulfuric acid (97%, 0.082 mL) was added dropwise at 5°C to a stirred solution of 3-carboxy-2,2,5,5-tetramethylpyrrolidine-1-oxyl (2.67 mmol) in methanol (2 mL). The reaction mixture was refluxed at 60°C for 2 h. After evaporation, ice water (10 mL) was added to the solution, which was then extracted with ether. The ether layer was dried with anhydrous magnesium sulfate. After removal of the solvent in a rotating evaporator, the residue was purified with silica gel column chromatography to give 1.45 mmol (54.4%).

[14N, D] IR (cm^{-1}): 1739 (C=O), 1201 (COO), Calculated for $C_{10}H_3D_{15}NO_3$: C, 55.72; H, 8.42; N, 6.50. Found: C, 56.67; H, 8.76; N, 6.59. [15N, D] IR (cm^{-1}): 1739 (C=O), 1200 (COO), Calculated for $C_{10}H_{18}{}^{15}NO_3$: C, 59.98; H, 9.06; N, 6.96. Found: C, 59.57; H, 9.08; N, 6.97. [15N, D] IR (cm^{-1}): 1739 (C=O), 1200 (COO), Calculated for

$C_{10}H_3D_{15}{}^{15}NO_3$: C, 55.47; H, 8.38; N, 6.47. Found: C, 51.92; H, 7.93; N, 5.88.

4-Hydroxyl-2,2,6,6-tetramethylpiperidine-1-oxyl (TEMPOL)

NaBH$_4$ (16.4 mmol) was added to a stirred solution of 4-oxo-2,2,6,6-tetramethylpiperidine-1-oxyl (65.6 mmol) in ethanol. The reaction mixture was stirred for 1 h in an ice bath. Brine was added to the solution, which was then extracted with ether. The ether layer was dried with anhydrous magnesium sulfate. After removal of the solvent in a rotating evaporator, the residue was first purified with silica gel column chromatography, and then recrystallized from a mixture of ether and hexane (2 / 1, v / v) to give an orange product.

[14N, D] IR (cm^{-1}): 3413 (-OH), Calculated for $C_9H_2D_{16}NO_2$: C, 57.34; H, 9.63; N, 7.44. Found: C, 59.31; H, 10.06; N, 7.57. [15N, H] IR (cm^{-1}): 3411 (-OH), Calculated for $C_9H_{18}{}^{15}NO_2$: C, 62.34; H, 10.47; N, 8.08. Found: C, 62.47; H, 10.52; N, 8.14. [15N, D] IR (cm^{-1}): 3413 (-OH), Calculated for $C_9H_2D_{16}{}^{15}NO_2$: C, 57.04; H, 9.57; N, 7.39. Found: C, 58.98; H, 9.99; N, 7.62.

ESR and OMRI experiments

The OMRI experiments were performed on a custom-built whole body scanner (Philips Research Laboratories, Hamburg, Germany) operating in a field-cycled mode to avoid excess power deposition during the ESR cycle. The nuclear magnetic resonance (NMR) field strength of the scanner is 15 mT and the NMR transmission chain operates at a frequency of 625 kHz using a saddle transmission coil. The receiving coil is a solenoid coil tuned to 625 kHz with a band-width of 80 kHz. The maximum transmission power is 250 W (peak). The ESR irradiation frequency is 226 MHz and a saddle coil is used for the transmission.

The corresponding DNP spectra of ^{14}N- and ^{15}N-labeled nitroxyl radicals were obtained by detecting the proton intensities after ESR irradiation in different magnetic fields in the range of 5 – 10 mT spanning the ESR spectra of the nitroxyl radicals. Enhancement factors of nitroxyl radicals were obtained from the image intensities divided by ESR non-irradiated (ESR OFF) image intensities. Enhancement factors were then correlated with the ESR line-widths of each nitroxyl radical. The ESR line-width was measured as the peak-to-peak line width using X-band ESR spectroscopy (Jeol, Akishima, Japan).

Phantom experiment

2 mM nitroxyl probes were contained in phantom tubes of various sizes. The inner diameters of these eight tubes were 7, 6, 5, 4, 3, 2, 1.5, and 0.7 mm. Typical scan conditions in OMRI were: repetition time (T_R)/echo time (T_E)/ESR irradiation time (T_{ESR}): 1,200 ms/25 ms/600 ms; no. of averages = 1; 64 phase-encoding steps. The image field of view, 48 mm, was represented by a 64×64 matrix.

References

[1] K. Yamada, T. Nakamura, H. Utsumi, *Free Radic. Res.* **2006**, *40*, 455 – 460.

[2] M. Yamato, T. Egashira, H. Utsumi, *Free Radic. Biol. Med.* **2003**, *35*, 1619 – 1631.

Arch. Pharm. Chem. Life Sci. 2008, *341*, 548–553

Nitroxyl Radicals for OMRI   553

[3] K. Takeshita, T. Takajo, H. Hirata, M. Ono, H. Utsumi, *J. Invest. Dermatol.* **2004**, *122*, 1463–1470.

[4] P. Kuppusamy, H. Li, G. Ilangovan, A. J. Cardounel, *et al.*, *Cancer Res.* **2002**, *62*, 307–312.

[5] K. I. Yamada, P. Kuppusamy, S. English, J. Yoo, *et al.*, *Acta Radiol.* **2002**, *43*, 433–440.

[6] A. Hirayama, K. Yoh, S. Nagase, A. Ueda, *et al.*, *Free Radic. Biol. Med.* **2003**, *34*, 1236–1242.

[7] A. Ueda, S. Nagase, H. Yokoyama, M. Tada, *et al.*, *Mol. Cell Biochem.* **2003**, *244*, 119–124.

[8] K. Yamada, I. Yamamiya, H. Utsumi, *Free Radic. Biol. Med.* **2006**, *40*, 2040–2046.

[9] A. W. Overhauser, *Phys. Rev.* **1953**, *92*, 411–412.

[10] M. C. Krishna, S. English, K. Yamada, J. Yoo, *et al.*, *Proc. Natl. Acad. Sci. U. S. A.* **2002**, *99*, 2216–2221.

[11] D. J. Lurie, D. M. Bussell, L. H. Bell, J. R. Mallard, *J. Magn. Reson.* **1988**, *76*, 366–370.

[12] K. Golman, J. S. Petersson, J. H. Ardenkjaer-Larsen, I. Leunbach, *et al.*, *J. Magn. Reson. Imaging* **2000**, *12*, 929–938.

[13] M. Alecci, I. Seimenis, S. J. McCallum, D. J. Lurie, M. A. Foster, *Phys. Med. Biol.* **1998**, *43*, 1899–1905.

[14] H. Utsumi, K. Yamada, K. Ichikawa, K. Sakai, *et al.*, *Proc. Natl. Acad. Sci. U. S. A.* **2006**, *103*, 1463–1468.

[15] D. Grucker, T. Guiberteau, B. Eclancher, J. Chambron, *et al.*, *J. Magn. Reson. B* **1995**, *106*, 101–109.

[16] E. G. Rozantsev, in *Free Nitroxyl Radicals*, Plenum Press, New York, **1970**.

[17] R. Seidemann, L. Dulog, *Makromol. Chem.* **1986**, *187*, 2545–2551.

[18] G. Sosnovsky, Z.-W. Cai, *J. Org. Chem.* **1995**, *60*, 3414–3418.

[19] H. Sano, K. Matsumoto, H. Utsumi, *Biochem. Mol. Biol. Int.* **1997**, *42*, 641–647.

[20] I. Nicholson, D. J. Lurie, F. J. L. Robb, *J. Magn. Reson.* **1994**, *104*, 250–255.